PREDICTION OF FORCE AND ACCELERATION CONTROL SPECTRA FOR SPACE SHUTTLE ORBITER SIDEWALL-MOUNTED PAYLOADS

By: Philip J. Hipol, The Aerospace Corporation

Keywords: Space Shuttle Sidewall, Vibration Testing, Finite Element Analysis, Apparent Weight

Abstract

The development of force and acceleration control spectra for vibration testing of Space Shuttle (STS) orbiter sidewall-mounted payloads requires reliable estimates of the sidewall apparent weight and free (i.e. unloaded) vibration during lift-off. The feasibility of analytically predicting these quantities has been investigated through the development and analysis of a finite element model of the STS cargo bay. Analytical predictions of the sidewall apparent weight were compared with apparent weight measurements made on OV-101, and analytical predictions of the sidewall free vibration response during lift-off were compared with flight measurements obtained from STS-3 and STS-4. These analyses suggest that the cargo bay finite element model has potential application for the estimation of force and acceleration control spectra for STS sidewall-mounted payloads.

Introduction

Vibration test criteria for Space Shuttle (STS) orbiter sidewall-mounted payloads were developed from accelerometer measurements obtained during launch of five STS flights [1]. These measurements were made at nine distinct locations on "hard" structure near the mounting points of payloads or orbiter equipment. Following traditionally accepted practices [2], the highest spectral density values of all vibration response measurements in the x-, y-, and z-axes were enveloped within the 20-2000 Hz range, resulting in the vibration test spectrum shown in Figure 1.

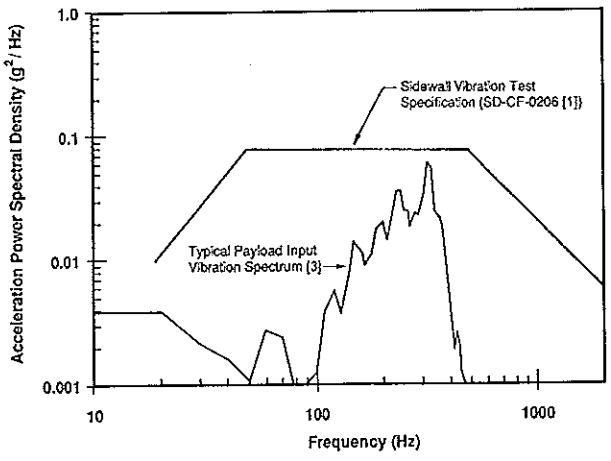

Figure 1. Sidewall Vibration Test Specification Compared with Typical Payload Input Vibration Spectrum [3]

Vibration test specifications derived in the manner described above have long been recognized to be conservative. This conservatism is due in part to the fact that the vibration response of an actual payload mounted on the sidewall will have peaks and notches, such that the actual vibration input to the payload will be much less than the specified vibration levels at most frequencies as illustrated in Figure 1. Overtesting at most frequencies is usually justified on the basis that the sidewall vibration test specification includes sufficient generality in order to be applicable to many different payloads and mounting locations.

Use of the sidewall vibration spectrum in a conventional acceleration-controlled vibration test may result in overtesting of the payload at significant base-fixed payload resonances [3-6]. This is due to the fact that in service, the apparent weight of the payload becomes large relative to the apparent weight of the mounting structure at significant payload resonances. The increased payload apparent weight loads the sidewall in a manner that causes a reduction of the vibration input to the payload. Conventional acceleration-controlled vibration tests do not allow the payload to load the shaker, thereby causing an overtest at significant payload resonances.

Typical methods for alleviating the risk of overtesting involve the reduction (or "notching") of the input acceleration spectrum at significant resonant frequencies in order to limit the vibration response of the payload. These methods are somewhat arbitrary, however, and allow for the possibility of undertesting. A more rigorous approach has recently been proposed which involves the control of both the acceleration and force during vibration testing [5,6]. One possibility is to employ an equation of the form:

$$\left|\frac{A_t}{(A_s)_{fr}}\right| + \left|\frac{F_t}{(F_s)_{bl}}\right| = 1 \qquad (1)$$

where A_t and F_t are the acceleration and force input to the test item, $(A_s)_{fr}$ is the free (i.e. unloaded) vibration of the mounting structure, and $(F_s)_{bl}$ is the blocked force of the mounting structure (i.e. the interface force required to hold the mounting structure motionless). The mounting structure free vibration and blocked force comprise acceleration control and force control spectra which are used to limit the response of the payload on the shaker in accordance with Equation (1).

The key to developing force and acceleration control spectra for vibration testing is the reliable estimation of envelopes for the mounting structure blocked force and free vibration. The free vibration of the mounting structure can be estimated from flight

measurements, whereas the mounting structure blocked force may be estimated through knowledge of the mounting structure apparent weight and free vibration [3,6], that is,

$$(F_s)_{bl} = W_s (A_s)_{fr} \qquad (2)$$

where W_s is the mounting structure apparent weight (i.e the applied force divided by the resulting acceleration in g's as a function of frequency).

The mounting structure apparent weight may be measured by impact hammer testing, however, experience with the STS orbiter sidewall [3] has found that these measurements may be difficult to obtain since it is necessary to excite the structure with adequate force in order to overcome non-linearities due to friction at joint interfaces. As a result, it is desirable to estimate the mounting structure apparent weight through analytical means. Linear analytical models are appropriate for the calculation of larger amplitude structural responses at a various payload mounting locations. The STS orbiter sidewall is particularly amenable to analytical predictions of this type since it has a relatively small number of locations on which to mount payloads.

This paper describes the development of a finite element model of the STS cargo bay (Figure 2) which was used to examine the feasibility of analytically predicting the sidewall apparent weight and free vibration during lift-off. Analysis results for the sidewall apparent weight are compared with apparent weight measurements made during ground tests of OV-101. The model is further extended for use in the prediction of the sidewall free vibration during lift-off, and analysis results are compared with vibration measurements obtained during lift-off of STS-3 and STS-4. Additional modeling refinements are then discussed relative to obtaining closer agreement between the analytical predictions and measurements of the sidewall apparent weight and free vibration.

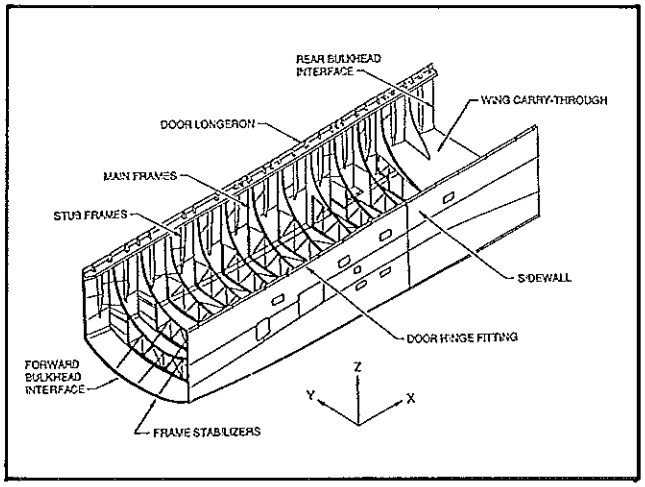

Figure 2. Cargo Bay Structural Elements [7]

Finite Element Model Development

The primary structural elements of the cargo bay include the sidewall, floor, frames, stabilizers, longerons, sill, and wing carry-through box as shown in Figure 2. Careful attention was given to modeling techniques in order to enhance the computational efficiency of the STS cargo bay finite element model, while maintaining sufficient fidelity to properly describe sidewall dynamic characteristics within the frequency range of interest. A brief description of these modeling techniques is provided below. A more detailed description of the cargo bay finite element model can be found in Reference [8].

Since the sidewall vibration test specification does not extend below 20 Hz, the cargo bay finite element model could be greatly simplified by the removal of low frequency fundamental bending modes of the orbiter which occur below 20 Hz. As a result, the wing, crew cabin, and engines were not included in the model as these were assumed to participate primarily in low frequency vehicle fundamental bending modes. The crew cabin and engines are connected to the cargo bay through the forward and aft bulkheads, which are heavily-stiffened structures comprised of integrally-machined aluminum panels. At these interfaces, boundary conditions were prescribed that constrained all translational motion at the sidewall and floor interfaces (Figure 3). The wings, which are connected to the sidewall at the upper and lower wing interface longerons, constrain sidewall normal displacements, as well as provide stiffness to the cargo bay for vertical bending deformations. Consequently, the wing was modeled with boundary conditions that constrained normal displacements of the sidewall at the upper and lower wing interface longerons only. Symmetric boundary conditions were imposed on the cargo bay centerline, as it was judged that the effects of these local constraints on the motion of the cargo bay floor would have a negligible effect on the sidewall vibration environment above 20 Hz.

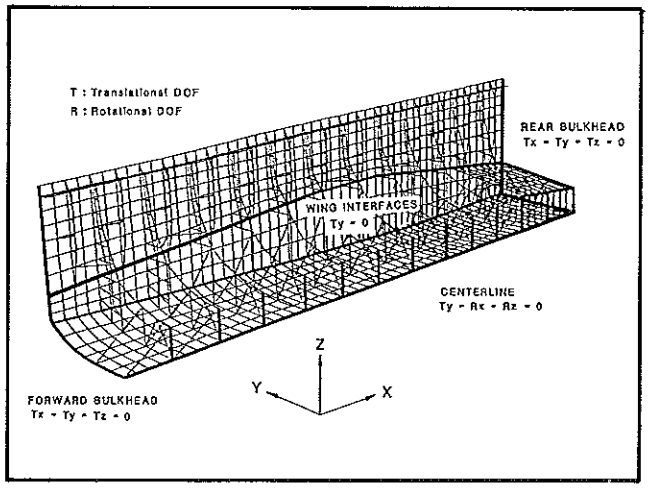

Figure 3. Boundary Conditions

The fidelity (or refinement) of the cargo bay finite element model was determined through consideration of maximum frequency requirements. The high frequency limit of the cargo bay finite element model was set to 200 Hz, since it is reasonable to expect that the fundamental resonances of most sidewall-mounted payloads will occur below this frequency. At 200 Hz, the minimum grid point separation distance for which a correlated pressure field could exist was determined to be roughly fourteen inches, corresponding to four finite elements in the orbiter x-direction between main frames. Modal analysis of a detailed sidewall panel verified that this mesh refinement was adequate to describe sidewall dynamic characteristics up to 200 Hz. This mesh refinement was adapted uniformly throughout the finite element model, resulting in 1335 grid points and 2491 elements (Figures 4 and 5). All sidewall surfaces were modeled flat and continuous, whereas the floor was modeled as a doubly curved surface in the x- and y-directions. All longerons, main frames, stub frames, truss structure, and stabilizers were included since these entities would have modes in the frequency range of interest, and would provide locations on which to mount sidewall payloads for future studies.

Much of the sidewall and floor consist of aluminum panels which are integrally stiffened by T-shape stringers which vary along the length of the cargo bay. The most accurate method for representing the integrally stiffened panels would involve modeling each of the individual stringers as offset beam elements on plates as wide as the stringer spacing. It can be seen, however, that such a model would become inordinately large, especially if the entire cargo bay is considered. In order to simplify the structural model, equivalent orthotropic plate properties were developed in which the stringer and panel properties were "smeared" in each of the in-plane panel directions. Mass properties for the equivalent orthotropic plates were obtained from weight estimates of the actual panels, considering a uniform distribution of the thermal protection system (TPS) tiles on the cargo bay exterior. Other non-structural masses on the sidewall and floor include tanks, plumbing, electrical, and thermal treatments, which were not included in the model since these were judged to influence only the low frequency fundamental bending modes (< 20 Hz).

The main frames and stub frames are essentially tapered I-beams consisting of integrally-machined aluminum flanges and webs. Rib-stiffened panels are used to connect each main frame to the sidewall, whereas truss members are used to connect each main frame to the floor. The frames are also connected at various locations to the sidewall and floor by truss members which act to stabilize the frames for out-of-plane deformation. Each stub frame and the upper portion of each main frame were modeled with bar elements defining the flanges, and plate elements defining the webs. The lower portions of each main frame were modeled with offset bar elements defining both the flanges and webs. All main frame truss members and frame stabilizers were modeled with rod elements, having no moment transfer capability.

The cargo bay doors are comprised of curved graphite/epoxy honeycomb panels and frames. Radiator panels are attached to the inner surfaces of the doors, whereas TPS tiles are applied to the outer surfaces. Load transfer among the doors, longeron, and sidewall is minimized by use of floating and shear hinges at the door/longeron interfaces. Since the doors do not stiffen the sidewall for bending deformations, they were greatly simplified in the finite element model. This was accomplished by modeling the doors (including radiator panels and TPS tiles) as distributed non-structural masses connected to the door longeron. Since the mass distribution of the doors on the longeron may influence sidewall lateral bending modes, future modeling efforts should consider statically reducing the cargo bay doors to the longeron in the appropriate degrees of freedom.

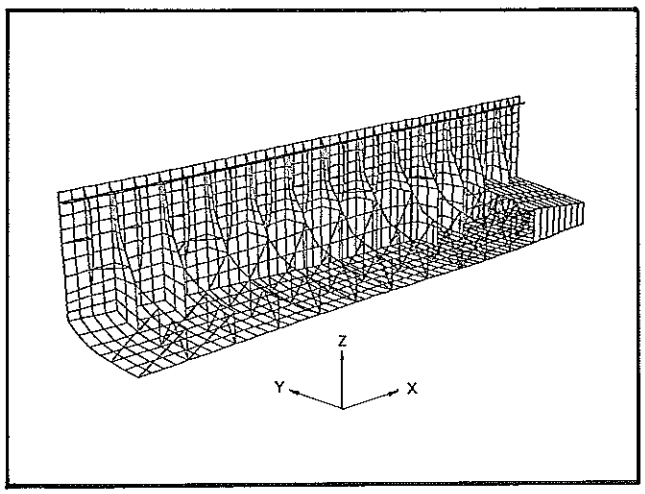

Figure 4. Half-Symmetry Finite Element Model

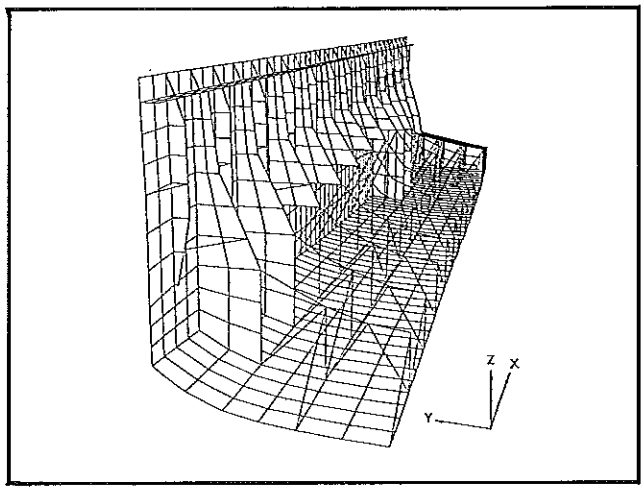

Figure 5. Half-Symmetry Finite Element Model

The cargo bay finite element model was partitioned into MSC/NASTRAN superelements (Table 1) in order to reduce computer storage, memory, and execution requirements [9]. The MSC/NASTRAN implementation of superelements essentially involves fixed boundary solutions of superelement components (or substructures) similar to that described in Reference [10]. Normal modes up to 400 Hz were calculated for each of the superelements defining the bays (Figure 6). This involved the extraction of approximately 120 normal modes for each of these superelements. The 400 Hz limit for the superelement component mode reduction was considered conservative in order to obtain fidelity up to 200 Hz for the entire system. Static reduction was performed for all superelements defining the stub frames (Figure 6) in order to remove about 80 normal modes from the model. It was considered reasonable to statically reduce the stub frames since their masses are typically small in comparison to the sidewall. All eight superelements were combined and assembled with the residual structure superelement, and system normal modes up to 200 Hz were calculated, involving the extraction of about 300 normal modes. An example cargo bay mode shape is given in Figure 7.

Table 1. Superelement Definition

Superelement	Description
Residual	Main Frames 3, 6, & 9
1	Bays 1, 2, & 3
2	Bays 4, 5, & 6
3	Bays 7, 8, & 9
4	Bays 10, 11, 12a, & 12b
5	Stub Frames 1, 2, & 3
6	Stub Frames 4, 5, & 6
7	Stub Frames 7, 8 & 9
8	Stub Frames 10, 11, 12a, & 12b

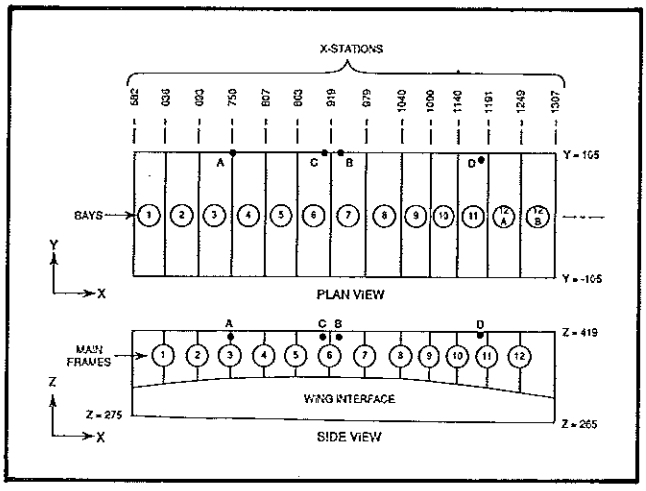

Figure 6. Cargo Bay Panels and Main Frames

Prediction of Sidewall Apparent Weight

The driving point apparent weight of the sidewall was calculated through a modal frequency response analysis in MSC/NASTRAN [11]. The driving point was defined at main frame #3 at station x=750, y=105, z=410 (location A" in Figure 6), corresponding to a location where apparent weight measurements were made during ground tests of OV-101 [3]. The analytical prediction of the apparent weight involved the application of a unit sinusoidal force normal to the sidewall finite element model at the driving point, and the calculation of the complex acceleration in the normal direction at the driving point as a function of frequency. The inverse of the driving point acceleration yields the driving point apparent weight. The magnitude and phase of the driving point apparent weight are given in Figures 8 and 9.

Comparison of the analytical prediction of the apparent weight magnitude with the apparent weight measurements at this location on OV-101 [3] indicates that there is reasonable agreement over the 20-200 Hz range (Figure 8). Discrepancies between the analytical prediction and measurements in the vicinity of 20 Hz are due to the fact that the analytical model did not include sufficient detail to predict low frequency vehicle bending modes. Discrepancies above 50 Hz are believed to be a result of using a constant loss factor of 0.08 in the finite element model. Past studies [12] have shown that a better approximation for the sidewall damping involves a loss factor which varies with the inverse of frequency as shown in Figure 10. Use of such a loss factor in the finite element model would tend to increase the apparent weight magnitude below 50 Hz, and decrease it above 50 Hz.

Comparison of the analytical prediction of the apparent weight phase with the OV-101 measurements shows roughly 15-125 degrees of phase shift over the 20-200 Hz range (Figure 9). The reason for this discrepancy is not well understood, however, the

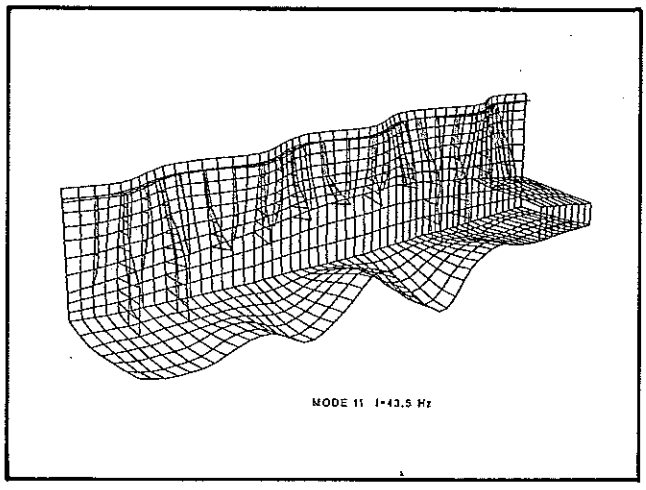

Figure 7. Example Cargo Bay Mode Shape

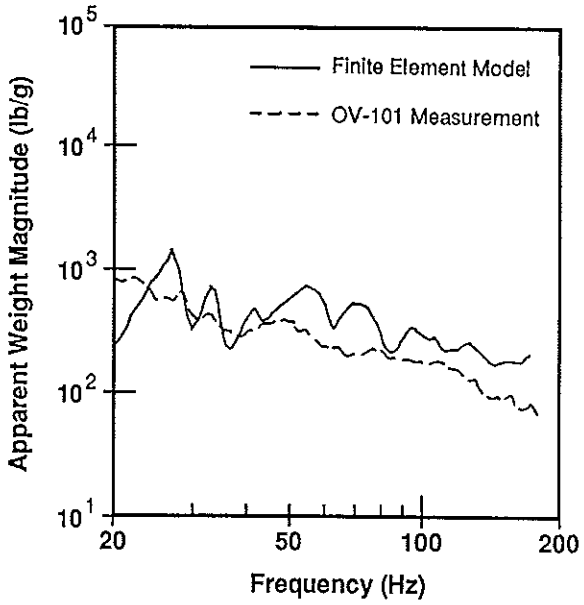

Figure 8. Sidewall Apparent Weight Magnitude

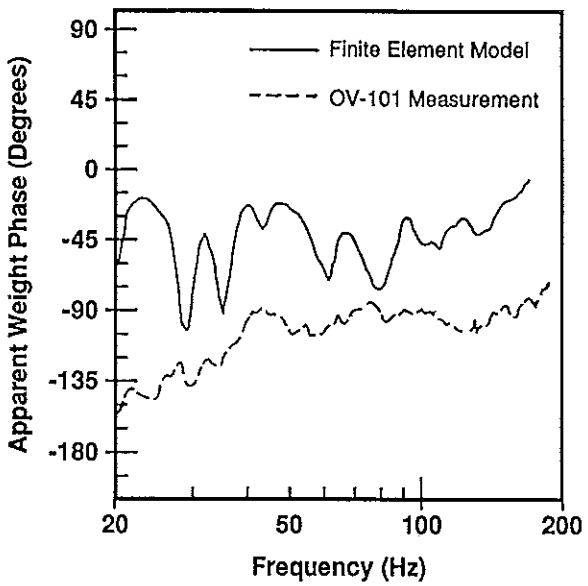

Figure 9. Sidewall Apparent Weight Phase

accurate representation of phase may not be important depending on the manner by which the force and acceleration control method is implemented. For example, if absolute values of the force and acceleration are used as shown in Equation (1), it is necessary to accurately represent the apparent weight magnitude only. Other methods for implementing force and acceleration control which may depend on the apparent weight phase will require further evaluation of the phase discrepancy in the cargo bay finite element model.

Prediction of Sidewall Free Vibration

The cargo bay finite element model can be used to obtain estimates of the sidewall free vibration response during lift-off in the event that flight measurements of the unloaded sidewall are not available at the desired payload mounting location. The prediction of the sidewall free vibration response employed the methodology described in References [13] and [14]. This methodology involved use of an efficient form of the equation:

$$G_{yy}(\omega) = \sum_{j=1}^{q} \sum_{i=1}^{q} H_{iy}(\omega)\, G_{ij}(\omega)\, H_{jy}(\omega)^{*T} \qquad (3)$$

where $G_{yy}(\omega)$ define elements of the auto spectrum of the structural accelerations at the response locations (y), $G_{ij}(\omega)$ is the spectral density matrix of the excitation pressure field, and $H_{iy}(\omega)$ and $H_{jy}(\omega)^{*T}$ are frequency response function matrices relating accelerations at the response locations (y) to discrete input forces applied to arbitrary points (i and j) on the sidewall structure.

Although the acoustic field acting on the orbiter during lift-off may be better described in terms of a convected pressure field [3,12], a reverberant excitation pressure field was assumed for simplicity. The cross-spectral density function for the excitation was assumed to be separable in the x-and z-directions [15], such that:

$$G_{ij}(\omega) = G_{pp}(\omega) \frac{\sin(k\Delta x)}{k\Delta x} \frac{\sin(k\Delta z)}{k\Delta z} \qquad (4)$$

where $G_{pp}(\omega)$ is the auto spectral density function of the excitation pressure field (assumed homogeneous), Δx and Δz are separation distances, and k is the wave number given by the radian frequency divided by the speed of sound.

The excitation pressure auto-spectral density function, $G_{pp}(\omega)$, was assumed to be uniform over the entire sidewall, and was obtained by averaging the auto spectral densities for the forward and aft regions of the sidewall described in the empirical model in Reference [12]. The resulting average value showed little frequency dependency in the frequency range of interest, allowing for the use of a constant value of 2966 $(N/m^2)^2/Hz$. The actual variation of the spectral density about this mean value was found to be less than ±1.3 dB.

The analytical prediction of the sidewall free vibration response assumed that the excitation pressure field was present only on the sidewall above the wing. This assumption was introduced primarily for computational convenience, and is justified by the analysis of Space Shuttle vibration data in Reference

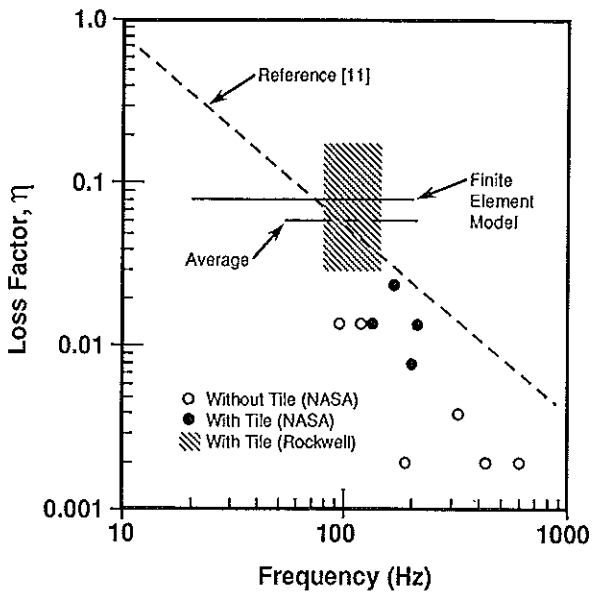

Figure 10. Sidewall Damping

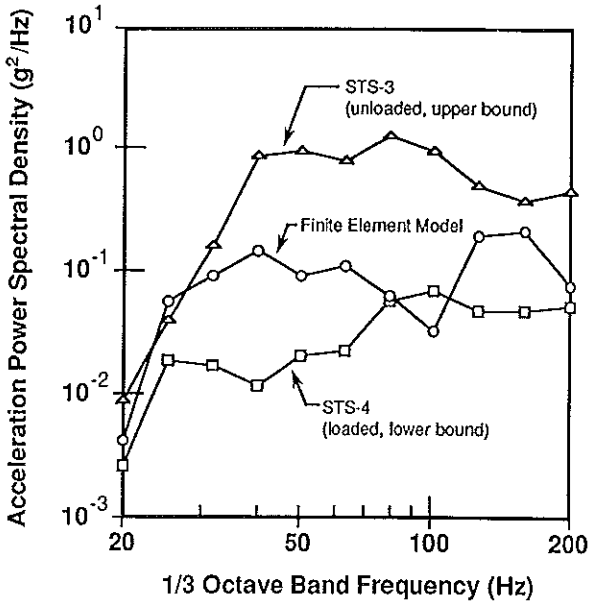

Figure 11. Sidewall Vibration Response at Lift-Off

[16]. This study found that even at low frequencies, the response of the sidewall in the y-direction was controlled by the acoustic pressure field acting on the sidewall above the wing, whereas the fluctuating pressure field on the cargo bay floor made a significant contribution to the motion of the sidewall in the z-direction only. A point on the sidewall at the longeron between the main frame and stub frame of bay #7 at station x=934, y=105, z=410 (location "B" in Figure 6) was selected to be the response point for the random vibration analysis. This location was chosen since it is an attachment interface location for a representative payload used in a subsequent study [3].

The predicted auto-spectral density function of the sidewall free vibration at the response location is shown plotted against acceleration spectra obtained from two early Space Shuttle launches (Figure 11). The flight acceleration spectra represents the maximum acceleration response of accelerometer V08D9349A at station x=908, y=105, z=410 on STS-3 (location "C" in Figure 6), and accelerometer V08D9388A at station x=1183, y=95, z=414 on STS-4 [16] (location "D" in Figure 6). The STS-3 flight data was obtained at the orbiter longeron, and was found to have much higher vibration levels than any of the other accelerometers on STS-3 or STS-4. This acceleration spectrum therefore represents the upper bound of the unloaded sidewall vibration response. The STS-4 flight data was obtained at a payload attachment trunnion location, and therefore represents the loaded sidewall vibration response. Comparison of the analytical prediction of the sidewall free vibration with the flight data shows that it is bounded by the flight data over much of the frequency range.

Summary and Conclusions

The development of force and acceleration control spectra for vibration testing of STS orbiter sidewall-mounted payloads requires reliable estimates of the sidewall apparent weight and free (i.e. unloaded) vibration during lift-off. The feasibility of analytically predicting these quantities has been investigated through the development and analysis of a finite element model of the STS cargo bay. Analytical predictions of the sidewall apparent weight were compared with apparent weight measurements made on OV-101, and analytical predictions of the sidewall free vibration response during lift-off were compared with flight measurements obtained from STS-3 and STS-4. These analytical predictions suggest that the cargo bay finite element model has potential application for the estimation of force and acceleration control spectra for STS sidewall-mounted payloads.

Further refinements of the cargo bay finite element model should be investigated before it is adapted for general use in the estimation of force and acceleration control spectra. These refinements include: (a) the use of a frequency-dependent form of the sidewall damping in order to obtain closer agreement with sidewall apparent weight measurements, (b) the development of a statically-reduced cargo bay door model in order to better represent the mass loading on the upper longeron, (c) the better representation of the acoustic field at lift-off in order to obtain closer agreement with sidewall free vibration measurements, and (d) revision of the current finite element model residual structure by inclusion of typical payload attachment interface locations to facilitate payload integration tasks.

Acknowledgements

This work was completed by the author while employed by Astron Research and Engineering, Santa Monica, CA, under California Institute of Technology/ Jet Propulsion Laboratory contract 958081, and United States Air Force Space Systems Division contract F04701-87-C-0010. The author wishes to acknowledge the contributions of Dr. John F. Wilby of Atlantic Applied Research Corporation, Van Nuys, CA, and Mr. Allan G. Piersol of Piersol Engineering Company, Woodland Hills, CA.

References

1. Anon., "Definition of SSV Structure-Borne Random Vibration Environment for DoD Payloads", SD-CF-0206, USAF Space Systems Division, Los Angeles, CA, January 1987.
2. Piersol, A. G., "The Development of Vibration Test Specifications for Flight Vehicle Components", *J. Sound Vib.*, Vol 4, No. 1, pp. 88-115, January 1968.
3. Wilby, J. F., Piersol, A. G., et al, "Vibration Test Procedures for Orbiter Sidewall-Mounted Payloads", Contract F04701-87-C-0010, USAF Space Systems Division, Los Angeles, CA, November 1988.
4. Smallwood, D. O., "The Application of Unloaded (Free) Motion Measurements and Mechanical Impedance to Vibration Testing", Proc. Institute of Environmental Sciences, pp. 71-82, April 1976.
5. Scharton, T. D., and Kern, D. L., "Using the VAPEPS Program to Support the TOPEX Spacecraft Design Effort", *59th Shock and Vibration Symposium*, Vol IV, pp. 21-36, Albuquerque, NM, December 1988.
6. Smallwood, D. O., An Analytical Study of a Vibration Test Method Using Extremal Control of Acceleration and Force", Proc. Institute of Environmental Sciences, pp. 263-271, 1989.
7. Anon., "Space Shuttle System Summary", SSV 74-32(R), Rockwell International, Downey, CA, May 1975.
8. Hipol, P. J., "Finite Element Model of the Space Shuttle Cargo Bay", Contract 958081, California Institute of Technology/Jet Propulsion Laboratory, Pasadena, CA, January 1988.
9. Anon., Handbook for Superelement Analysis, MacNeal-Schwendler Corporation, Los Angeles, CA, 1982.
10. Craig, R. R., and Bampton, M. C. C., "Coupling of Substructures for Dynamic Analysis", *AIAA J.*, Vol. 6, No. 7, July 1968.
11. Anon., Handbook for Dynamic Analysis, MacNeal-Schwendler Corporation, Los Angeles, CA, 1983.
12. Pope, L. D. and Wilby, J. F., "Space Shuttle Payload Bay Acoustics Prediction Study", Contract NAS5-22832, NASA Goddard Space Flight Center, Greenbelt, MD, March 1980.
13. Hipol, P. J. and Piersol, A. G., "Efficient Implementation of Random Pressure Fields with the Finite Element Method", SAE 871740, *SAE Aerospace Technology Conference*, Long Beach, CA, October 1987.
14. Hipol, P. J., "Finite Element Prediction of Vibro-Acoustic Environments", SAE 892371, *SAE Aerospace Technology Conference*, Anaheim, CA, September 1989.
15. Morrow, C. T., "Point-to-Point Correlation of Sound Pressures in Reverberant Chambers", Shock and Vibration Bulletin, No. 39, 1969.
16. Wilby, J. F. and Piersol, A. G., "An Evaluation of Shuttle Vibration at Payload Attachments During Lift-Off", Contract MH-827659, California Institute of Technology/Jet Propulsion Laboratory, Pasadena, CA, August 1987.